行政院國家科學委員會專題研究計畫　成果報告

(Ln1-xAxMn1-yBy03)磁傳輸特性及多層膜交換偏壓機制的探討

計畫類別：個別型計畫
計畫編號：NSC93-2112-M-164-002-
執行期間：93 年 08 月 01 日至 94 年 07 月 31 日
執行單位：修平技術學院電機工程系

計畫主持人：陳宏仁

計畫參與人員：許進添，高銘政，林宸澂

報告類型：精簡報告

處理方式：本計畫可公開查詢

中　華　民　國 94 年 10 月 27 日

行政院國家科學委員會補助專題研究計畫■ 成 果 報 告
□期中進度報告

計畫名稱： (Ln1-xAxMn1-yByO3)磁傳輸特性及多層膜交換偏壓機制的探討

計畫類別：■個別型計畫　　□ 整合型計畫
計畫編號：NSC 93－2112－M－164－002－
執行期間：93 年 08 月 01 日至 94 年 07 月 31 日

計畫主持人：陳宏仁教授兼工程學群召集人
共同主持人：
計畫參與人員：許進添，高銘政，林宸澂

成果報告類型(依經費核定清單規定繳交)：■精簡報告　□完整報告

本成果報告包括以下應繳交之附件：
□赴國外出差或研習心得報告一份
□赴大陸地區出差或研習心得報告一份
■出席國際學術會議心得報告及發表之論文各一份
□國際合作研究計畫國外研究報告書一份

處理方式：除產學合作研究計畫、提升產業技術及人才培育研究計畫、列管計畫及下列情形者外，得立即公開查詢
□ 涉及專利或其他智慧財產權，■一年□二年後可公開查詢

執行單位：修平技術學院

中　華　民　國　94　年　10　月　26　日

行政院國家科學委員會專題研究計畫成果報告

(Ln1-xAxMn1-yByO3)磁傳輸特性及多層膜交換偏壓機制的探討

The study of magnetotransport properties of (Ln1-xAxMn1-yByO_3) and its exchange bias mechanism of multi-layer films

計畫編號：NSC 93-2112-M-164-002-

執行期限：93 年 8 月 1 日至 94 年 7 月 31 日

主持人：陳宏仁教授兼工程學群召集人　　修平技術學院電機工程系

計畫參與人員：許進添，高銘政，林宸澂

1. Abstract

此計畫主要對於 $La_{0.7-x}Ln_xPb_{0.3}MnO_3$ (Ln = Pr, Nd, Gd, Dy, Sm and Y)錳化合物的磁化行為作綜合性探討。La 離子被 Pr，Nd，Gd，Dy，Sm 或 Y 取代將導致降低鐵磁有序溫度 T_c 及在場冷卻(FC)-零場冷卻(ZFC)量測中顯示具一個短程有序自旋相。這主要乃相對於 La 離子 Pr，Nd，Gd，Dy，Sm 及 Y 離子具有較小的離子半徑，取代後造成鈣鈦礦結構較大的扭曲。由研究結果可獲得飽和磁化率 Ms 隨著 Po 或 Na 含量的增加而增加，卻隨著 Sm 或 Y 含量的增加而降低。然而，Gd 及 Dy 含量的增加卻使得 Ms 先增加後再降低。此結果可以用具 *f*-shell 電子之磁性離子及較小離子半徑兩種競爭特性來解釋鐵磁性的增加或降低。

關鍵字：鈣鈦礦結構，飽和磁化率，鐵磁性，自旋。

The magnetization behaviors of perovskite oxides, $La_{0.7-x}Ln_xPb_{0.3}MnO_3$ (Ln=Pr, Nd, Gd, Dy, Sm and Y), have been synthesized. The replacement of La ion by Pr, Nd, Gd, Dy, Sm or Y results in a considerable decrease in the ferromagnetic ordering temperature T_c and clearly irreversible behavior in the FC-ZFC curves showing a short-range spin order phase. The fact is in agreement with the smaller ionic radii of Pr, Nd, Gd, Dy, Sm and Y ions in contrast to La ion and the corresponding larger distortion of perovskite structures. The saturation magnetization M_S increases as Pr or Nd content increases while M_S decreases as Sm or Y content increases. Moreover, the saturation magnetization M_S increases and then decreases as Gd and Dy content increases. These results can be explained in terms of the competition between the increase of ferromagnetically interacting spins due to the introduction of magnetic Pr or Sm ions with *f*-shell electrons and suppression of ferromagnetism due to structure tuning induced by the small ionic radius of the interpolated cation into the La-site.

Keywords：perovskite structures, saturation magnetization, ferromagnetism, spin.

2. Introduction

Manganese oxides, $A_{1-x}A'_xMnO_3$ (A = La, Pr, Nd, Gd, Dy, Sm, Y etc., and A' = Ca, Sr, Ba, Pb etc.), with ABO_3 perovskite structure have attracted considerable investigation because of the discovery of

colossal magnetoresistance (CMR) effect accompanied with rich variety of magnetic and electrical properties (1-9). The partial substitution of divalent ions for the trivalent rare earth ions induces ferromagnetism in these compounds due to the conversion of Mn^{3+} ($t_{2g}^3e_g^1$) into Mn^{4+} ($t_{2g}^3e_g^0$) explained by double exchange (DE) interaction (10-11) with additional polaronic and Jahn-Teller effects (12). These oxides show transitions from paramagnetic to ferromagnetic state in magnetism and insulating to metallic state in electricity with the decrease of temperature. There appears to be a direct relationship between the complex lattice effects and the physical properties in these perovskite compounds (13). The introduction of lanthanide ion, such as Pr, Nd, Gd, Dy, Sm and Y etc., smaller than La into the perovskite, $La_{0.7-x}Ln_xA'_{0.3}MnO_3$, is expected to produce a deformation of the octahedral MnO_6 that results in a modified Mn-O-Mn bond angle and in a consequence reduction of the DE interaction between Mn^{3+} and Mn^{4+}. In the paper, we have made a comparative study of the influence on the magnetic properties induced by La^{3+} site substitution. To evaluate the effect of rare-earth element substitution on magnetic properties, we have studied a series of samples in which La^{3+} is partially replaced by Pr^{3+}, Nd^{3+}, Gd^{3+}, Dy^{3+}, Sm^{3+} or Y^{3+} with the Mn^{3+}/Mn^{4+} ratio fixed at 0.7/0.3 and the mean radius of the A-site ions is systematically decreased in these $La_{0.7-x}Ln_xPb_{0.3}MnO_3$ compounds.

3. Experimental

Polycrystalline bulk samples of the compounds, $La_{0.7-x}Ln_xPb_{0.3}MnO_3$ (Ln=Pr, Nd, Gd, Dy, Sm and Y), were prepared by conventional ceramic fabrication technique of solid-state reaction. After wet-milled by SPEX 8000M, well-dried hyperfine powders, Ln_2O_3 (99.95% purity, Ln= Nd, Gd, Dy, Sm and Y), Pr_6O_{11} (99.95% purity), $PbCO_3$ (99.99% purity) and $MnCO_3$ (99.99% purity), were mixed by Retsch Mix Miller MM-2000 in a stoichiometric ratio and calcined in air at 800°C for 24 hours with intermediate grindings three times. After grinding, the mixed powders were pressed into a disk-shape pellet with a diameter of 12 mm and a thickness of 2 mm. The disk samples were sintered in air at 1200°C for 72 hours and then cooled down to room temperature at a cooling rate of 3°C/min. The structure and phase purity of the samples were examined by X-ray diffraction with Cu-K α radiation. The magnetization measurements between 5 K and 350 K were performed in a quantum designed superconducting quantum interference device MPMS-5S SQUID magnetometer. The zero-field cooling (ZFC) and field cooling (FC) curves were taken under an applied field of 100 Oe. Temperature dependence of magnetization curves in an applied field of 50 kOe ere also recorded from 5 K to 350 K.

4. Results and Discussion

The magnetization behaviors of perovskite oxides, $La_{0.7-x}Ln_xPb_{0.3}MnO_3$ (Ln=Pr, Nd, Gd, Dy, Sm and Y), have been

synthesized. The size mismatch effect occurs when the Ln-site ions are smaller than La to fill the space in the octahedral MnO_6 and, consequently, results in a more distorted structure and Mn-O-Mn bond bending (14). The ionic radii and electronic configuration of Pr, Nd, Gd, Dy, Sm and Y are listed in Table 1 (15). Hence, it is interest for us to survay the distortion effect induced by La-site substitution on the magnetic behavior.

In order to exam the spin order and magnetic behavior, we measured the ZFC and FC magnetization curves in a low field of 100 Oe. Low field ZFC-FC magnetization measurement is one of the methods generally used to characterize short-range spin order or long-range spin order behaviors. The ZFC and FC curves of all samples are presented in Fig. 1. For x = 0 compounds of all systems, the ZFC and FC magnetization curves, except at very low temperature, are almost overlap indicating a ferromagnetic long-range spin order. Conversely, the irreversibility is found for Ln-site substituted compounds, and indicates the existence of short-range spin order. In these Ln-site substituted compounds, the ZFC curves coincide with the FC curves at high temperature, but separate as ths temperature decreases below ferromagnetic-paramagnetic transition temperature T_C (defined as the temperature where the slop, $|dM/dT|$, reaches a maximum value calculated from the ZFC curve). In pure manganite, the local clustering of the Mn^{3+} ions aroung the Mn^{4+} ones eventually leads to a ferromagnetic spin order of long-range type. For the Ln-site substituted phases, the smaller radius of the introduced Ln cation generates a distortion in the cell which leads the zigzagging of the MnO_6 octahedra containing the manganese atoms. As a result, the Mn-O-Mn angle decreases and the ferromagnetic DE interaction suppresses. Thus, the substitution of La by Pr, Nd, Gd, Dy, Sm or Y results in a considerable decrease of T_C due to the effect of lattice distortion and Mn-O-Mn bonds bending induced by substituting smaller lanthanide ions for La ion.

Figure 2 shows the temperature dependence of magnetization curves measured in an applied field of 50 kOe for the $La_{0.7-x}Nd_xPb_{0.3}MnO_3$ and $La_{0.7-x}Pr_xPb_{0.3}MnO_3$ oxide systems. The samples undergo a paramagnetic to ferromagnetic transition as the temperature decreases. For both of the two systems, the saturation magnetization (M_S, defined as the magnetization at 5 K and an applied field of 50 kOe for comparison) increases with the increase of Nd or Pr content. In the Nd-doped compounds, the manganese sublattice is ferromagnetic and the magnetic ions, Nd^{3+}, with *f*-shell electrons are gradually aligned with manganese as the temperature decreases. The rare earth magnetic ions Nd^{3+} contribute to an additional magnetization value to the total moment for Nd-doped samples. However, the Nd^{3+}, with *f*-shell electrons (electronic configuration as listed in Table 1) are hard to be fully aligned with the manganeses due to the deformation induced by the substitution of Nd for La (radii as listed in Table 1). As Fig. 2(a) shows, complete magnetic saturation for Nd-doped samples is not achieved even at 5 K, which

shows high dM/dT slope. For the Pr-doped compounds, similar behavior was also observed. However, due to the less unpaired *f*-shell electrons of Pr^{3+} than Nd^{3+}, the M_S values are smaller of Pr-doped compounds than those of Nd-doped ones as shown in Fig. 2(a) and (b).

The temperature dependence of magnetization curves measured in an applied field of 50 kOe for the $La_{0.7-x}Gd_xPb_{0.3}MnO_3$ and $La_{0.7-x}Dy_xPb_{0.3}MnO_3$ oxide systems are shown in Fig. 3. The samples also perform a paramagnetic to ferromagnetic transition as the temperature decreases. For both of the two systems, the M_S increases initially with the increase of Gd or Dy content, reaches a maximum value for x = 0.1 and then decreases with the increase of Gd or Dy content. The magnetic behaviors of Gd-doped and Dy-doped are dissimilar from that of Nd-doped and Pr-doped. The results can be explained in terms of the competition between the increase of ferromagnetically interacting spins and suppression of ferromagnetism. As listed in Table 1, the effective moment values of Gd^{3+} and Dy^{3+} are quite larger than that of La^{3+}, Pr^{3+} and Nd^{3+} and in a consequence the Gd^{3+} or Dy^{3+} contribute to a more additional magnetization value to the total moment than Pr^{3+} and Nd^{3+}. This is the reason why M_S increases with the increase of Gd or Dy content due to the increase of ferromagnetically interacting spins initially. However, the radii of Gd^{3+} and Dy^{3+} are quite smaller than La^{3+}, Pr^{3+} and Nd^{3+}. The introduction of Gd or Dy into La site induces heavy distortion of crystal structure and suppression of ferromagnetism. Complete magnetic saturation for Gd-doped and Dy-doped samples are not achieved even at 5 K. The higher dM/dT slope values for heavy doped samples show that the suppression of ferromagnetism induced by structure distortion plays a primary role. Thus, the M_S decreases with the increase of doped content for $x \geqq 0.1$.

In contrast, M_S decreases with the increase of Sm or Y content in the Sm-doped and Y-doped oxids as shown in Fig. 4. It can be inferred that the substitution of smallest Sm^{3+} or Y^{3+} for La^{3+} can distort the perovskite structure and give rise to a larger bending angle of the Mn-O-Mn, which consequently weakens the ferromagnetic double exchange interaction between Mn^{3+} and Mn^{4+}. The different magnetization processes of the two system can be ascribed to a competition in these compounds between suppression of ferromagnetism induced by lattice distortion and increase of ferromagnetically interacting spins due to the introduction of magnetic Ln^{3+} ions with *f*-shell electrons. The effective magnetic moments are 0.84 μ_B for Sm^{3+} and 0 μ_B for Y^{3+}, which is much smaller than those of Pr^{3+}, Nd^{3+}, Gd^{3+} and Dy^{3+}. Therefore, the increase of ferromagnetism suppression induced by structure distortion with the increase of Sm or Y content plays a major role in the competition for Sm-doped and Y-doped compounds and which is quite different from that of the rest compounds.

5. Conclusions

In summary, we have carried out the

magnetization measurement of the perovskite oxides, $La_{0.7-x}Ln_xPb_{0.3}MnO_3$ (Ln=Pr, Nd, Gd, Dy, Sm and Y) to study the substitution effect of La-site on the magnetic behavion. The magnetization behavior of (Nd, Pr)-doped systems is dissimilar to (Gd, Dy)-doped or (Sm, Y)-doped systems. The dissimilar magnetic behavior of these three systems can be interpreted in terms of the competition between increase of ferromagnetically interacting spins due to the introduction of magnetic lanthanide ions with *f*-shell electrons and suppression of ferromagnetism induced by lattice distortion. This work was sponsored by the National Science Council of the Republic of China under the grants No. NSC 93-2112-M-164-002-.

6. References

1. J.J. Neumeier and J.L. Cohn, Physical Review B, 61, 14319 (2000).
2. S. Roy and N. Ali, Journal of Applied Physics, 89, 7425 (2001).
3. C. Mitra, P. Raychaudhuri, J. John, S.K. Dhar, A.K. Nigam, and R. Pinto, Journal of Applied Physics, 89, 524 (2001).
4. S.L. Young, Y.C. Chen, H.Z. Chen, L. Horng and J.F. Hsueh, Journal of Applied Physics, 91, 8915 (2002).
5. N. Shannon and A.V. Chubukov, Physical Review B, 65, 104418 (2002).
6. G.T. Tan, S. Dai, P. Duan, Y.L. Zhou, H.B. Lu, and Z.H. Chen, Physical Review B, 68, 014426 (2003).
7. P. Duan, G. Tan, S. Dai, Y. Zhou and Z. Chen, Journal of Physics: Condense Matter, 15, 4469 (2003).
8. S. Zhang, L. Luan, S. Tan and Y. Zhang, Physical Review Letter, 84, 3100 (2004).
9. J.M. De Teresa, M.R. Ibarra, J. Garcia, J. Blasco, C. Ritter, P.A. Algarabel, C. Marquina, and A. del Moral, Physical Review Letter, 76, 3392 (1996).
10. C. Zener, Physical Review, 82, 403 (1951).
11. A.N. Ulyanov, S.C. Yu, N.Y. Starostyuk, N.E. Pismenova, Y.M. Moon and K.W. Lee, Journal of Applied Physics, 91, 8900 (2002).
12. A.J. Millis, B.I. Shraiman and R. Mueller, Physical Review Letter, 77, 175 (1996).
13. H. Itoh, T. Ohsawa, and J. Inoue, Physical Review Letter, 84, 2501 (2000).
14. H.Y. Hwang, S-W. Cheong, P.G. Radaelli, M. Marezio and B. Batlogg, Physical Review Letter, 75, 914 (1995).
15. R.D. Shannon, Acta. Cryst. A, 32, 751 (1976).

Table 1 Values of radius, electronic configuration, effective moment and magnetism for trivalent lanthanide and yttrium ions (15).

Ion	Radius (nm)	Electronic configuration	Effective moment (μ_B)	Magnetism
La^{3+}	0.136	[Xe]	0	nonmagnetic
Pr^{3+}	0.130	$[Xe](4f)^2$	3.58	magnetic
Nd^{3+}	0.127	$[Xe](4f)^3$	3.62	magnetic
Sm^{3+}	0.124	$[Xe](4f)^5$	0.84	magnetic
Gd^{3+}	0.122	$[Xe](4f)^7$	7.94	magnetic
Dy^{3+}	0.120	$[Xe](4f)^9$	10.63	magnetic
Y^{3+}	0.119	[Kr]	0	nonmagnetic

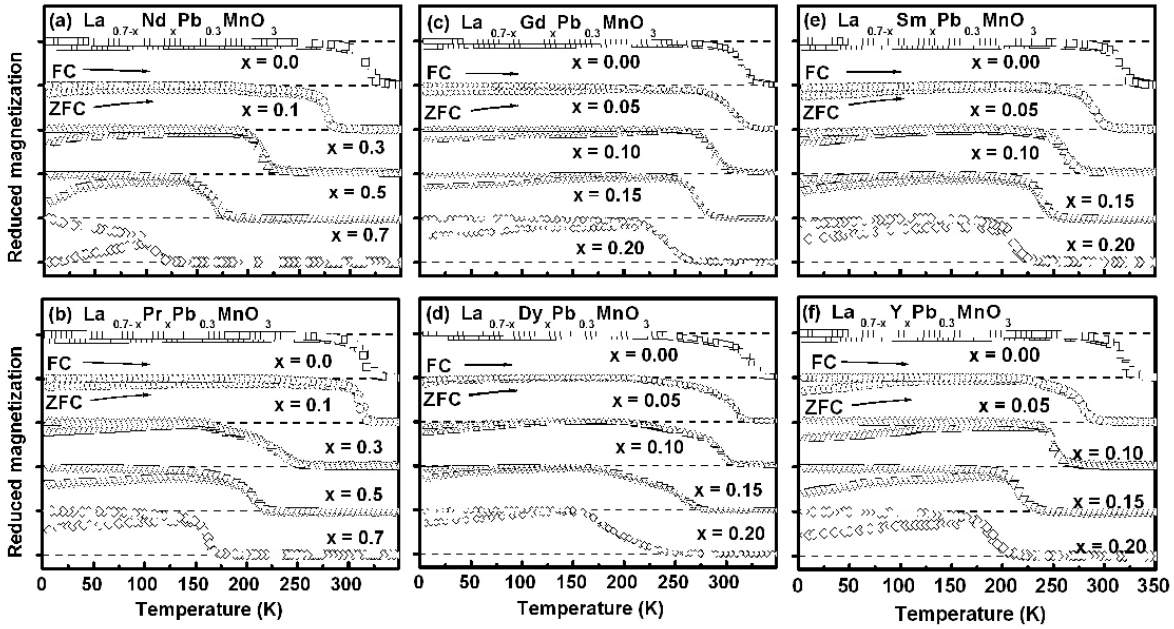

Fig. 1 Temperature dependence of zero-field cooling and field cooling magnetization curves for all systems.

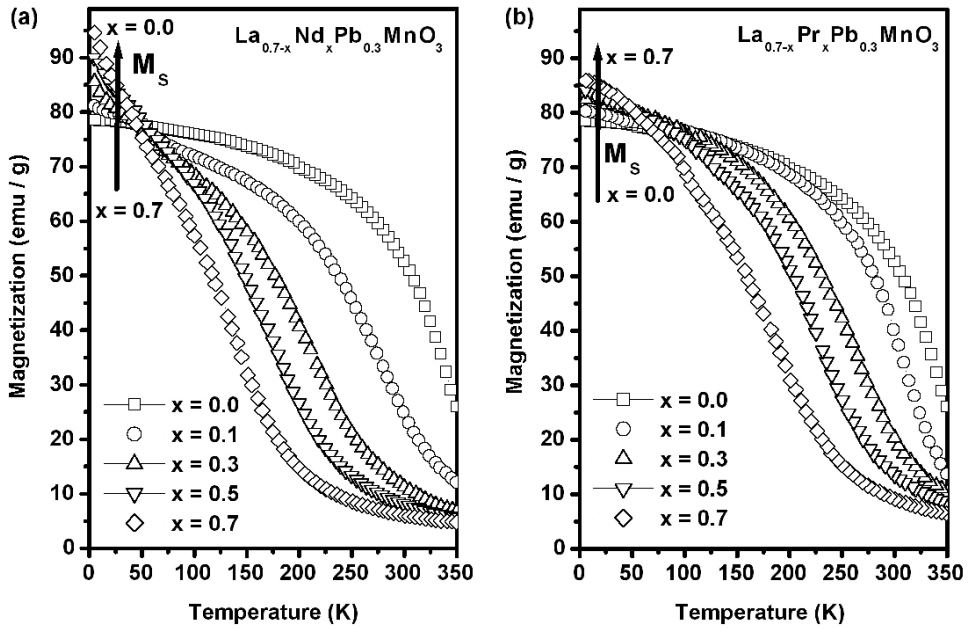

Fig. 2 Temperature dependence of magnetization curves measured in an applied field of 50 KOe for the (a)$La_{0.7-x}Nd_xPb_{0.3}MnO_3$ and (b)$La_{0.7-x}Pr_xPb_{0.3}MnO_3$ oxide systems.

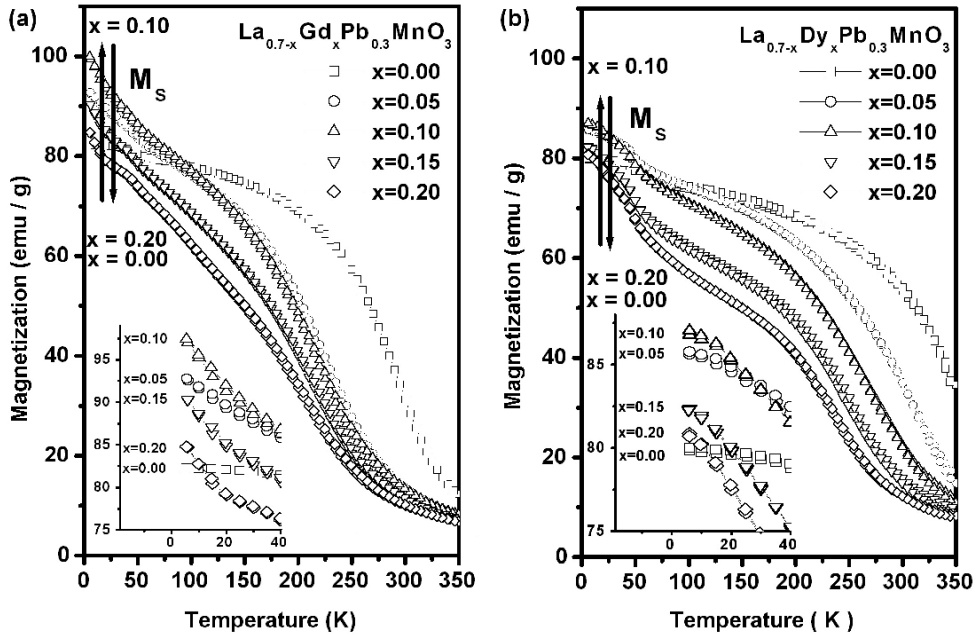

Fig. 3 Temperature dependence of magnetization curves measured in an applied field of 50 KOe for the (a)$La_{0.7-x}Gd_xPb_{0.3}MnO_3$ and (b)$La_{0.7-x}Dy_xPb_{0.3}MnO_3$ oxide systems.

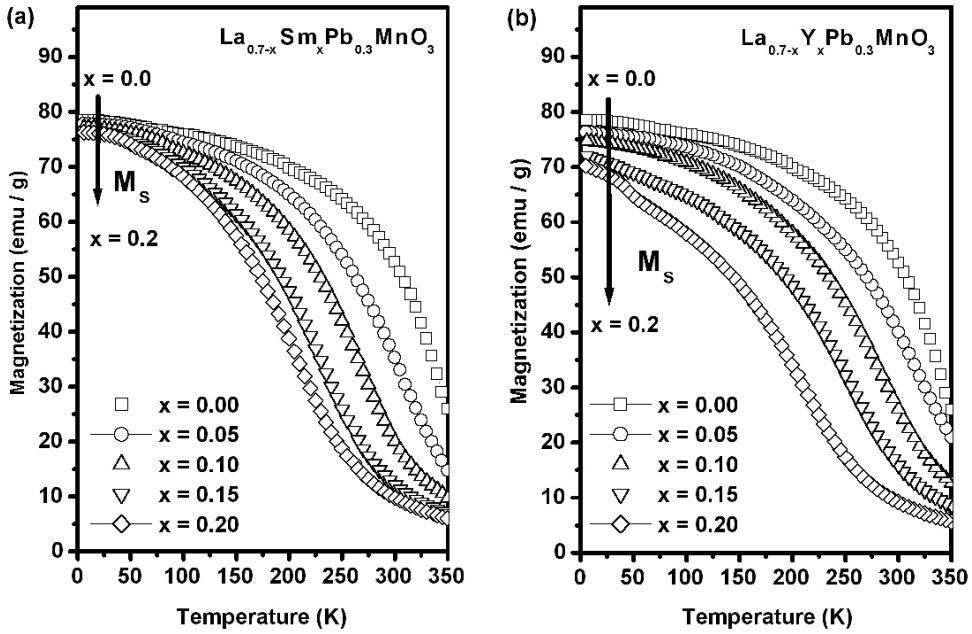

Fig. 4 Temperature dependence of magnetization curves measured in an applied field of 50 KOe for the (a)$La_{0.7-x}Sm_xPb_{0.3}MnO_3$ and (b)$La_{0.7-x}Y_xPb_{0.3}MnO_3$ oxide systems.